Electronic Supplementary Material (ESI) for Nanoscale.

Dual magnetic field and temperature optical probes of controlled crystalline phases in lanthanide-doped multi-shell nanoparticles

Flavia de Sousa Ferreira,[a] Amanda Justino de Morais,[a] Claudia Manuela Santos Calado,[a] Fernando Iikawa,[b] Odilon D. D. Couto Junior,[b] Gabriel Brunet,[c] Muralee Murugesu,[c] Italo O. Mazali,[a] Fernando A. Sigoli*

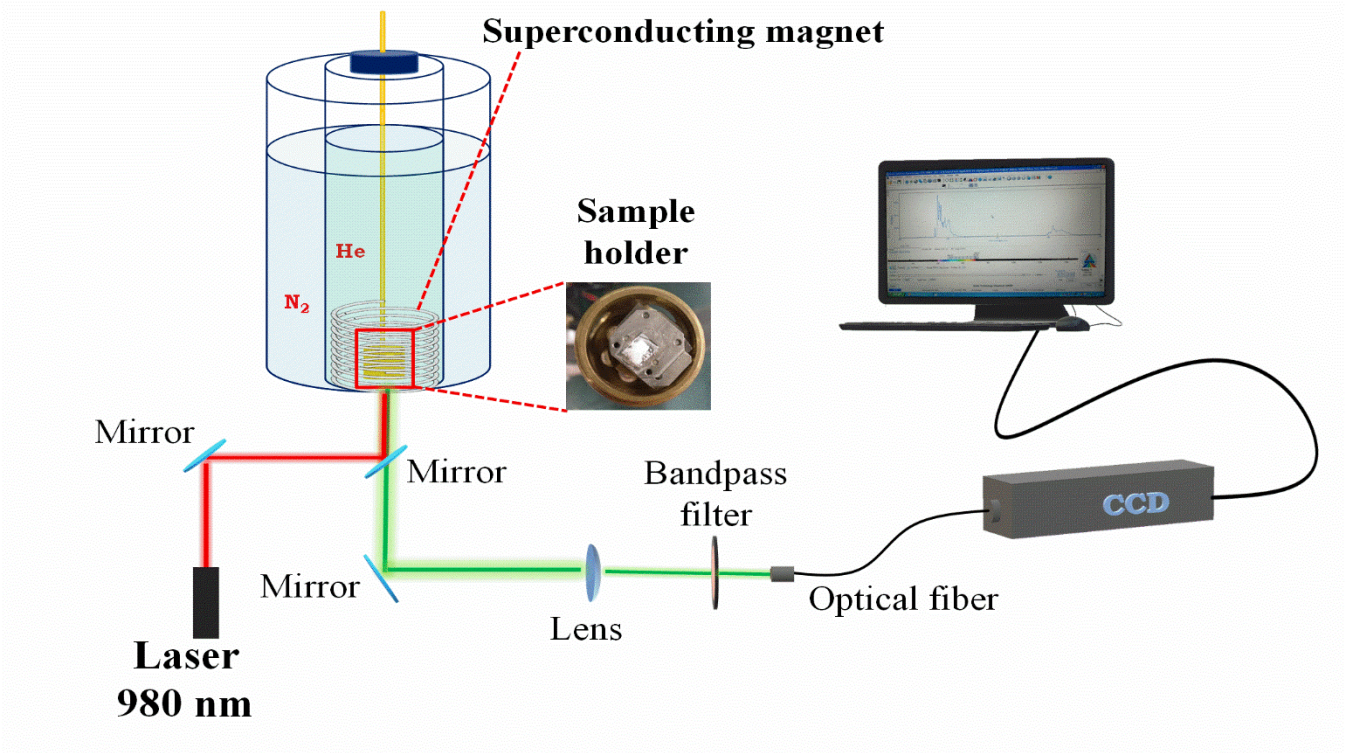

Scheme 1*:* Scheme of the experimental setup for the photoluminescence measurement under an applied magnetic field.

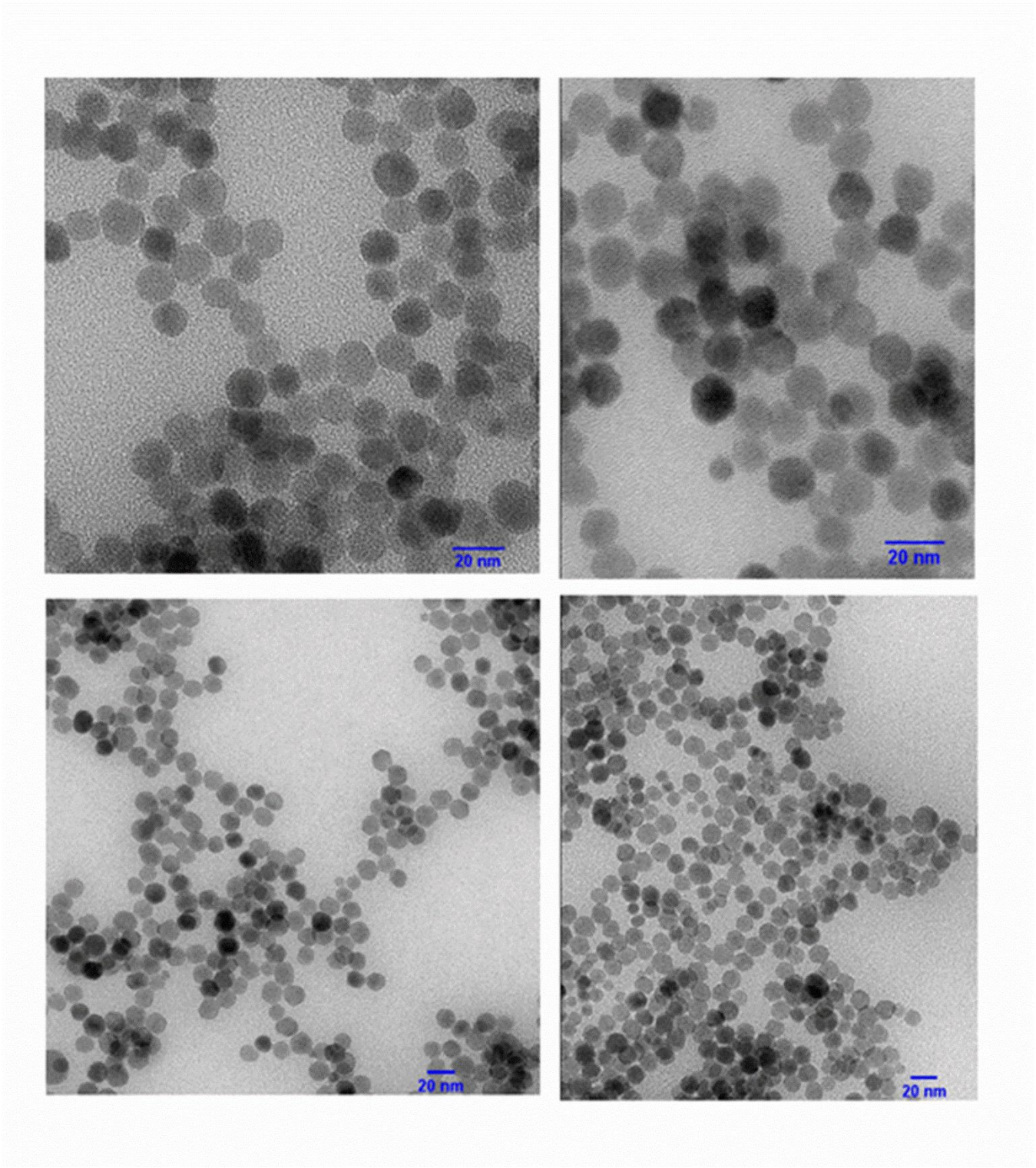

Figure S1. Bright Field TEM images of the α-$NaY_{0.85}Dy_{0.15}F_4$@α-$NaYF_4$@β-$NaGd_{0.80}Er_{0.02}Yb_{0.18}F_4$ @β-$NaGd_{0.75}Nd_{0.25}F_4$ core@multi-shell nanoparticles.

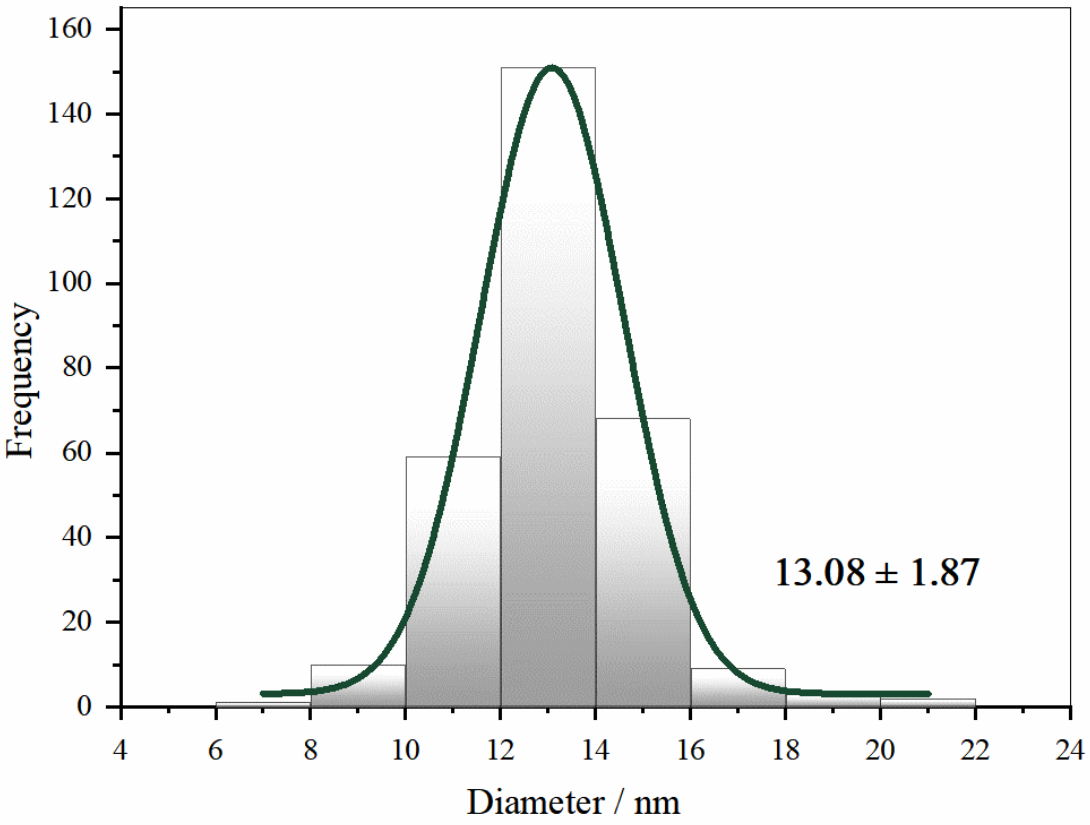

Figure S2. Particle size histogram and Gaussian fitting (green) of the α-$NaY_{0.85}Dy_{0.15}F_4$@ α-$NaYF_4$@β-$NaGd_{0.80}Er_{0.02}Yb_{0.18}F_4$ @β-$NaGd_{0.75}Nd_{0.25}F_4$ core@multi-shell nanoparticles.

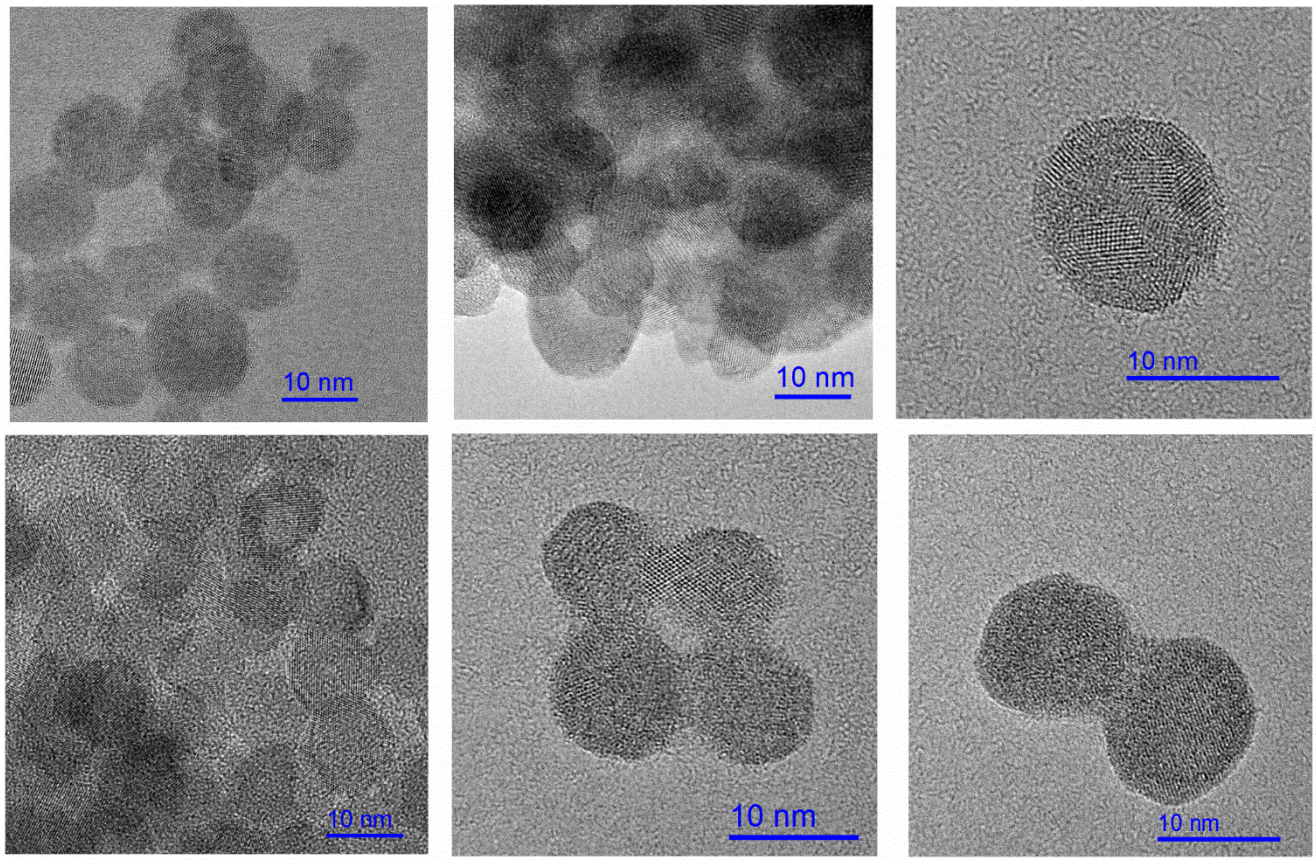

Figure S3. High resolution TEM of the α-$NaY_{0.85}Dy_{0.15}F_4$@ α-$NaYF_4$@β-$NaGd_{0.80}Er_{0.02}Yb_{0.18}F_4$ @β-$NaGd_{0.75}Nd_{0.25}F_4$ core@multi-shell nanoparticles.

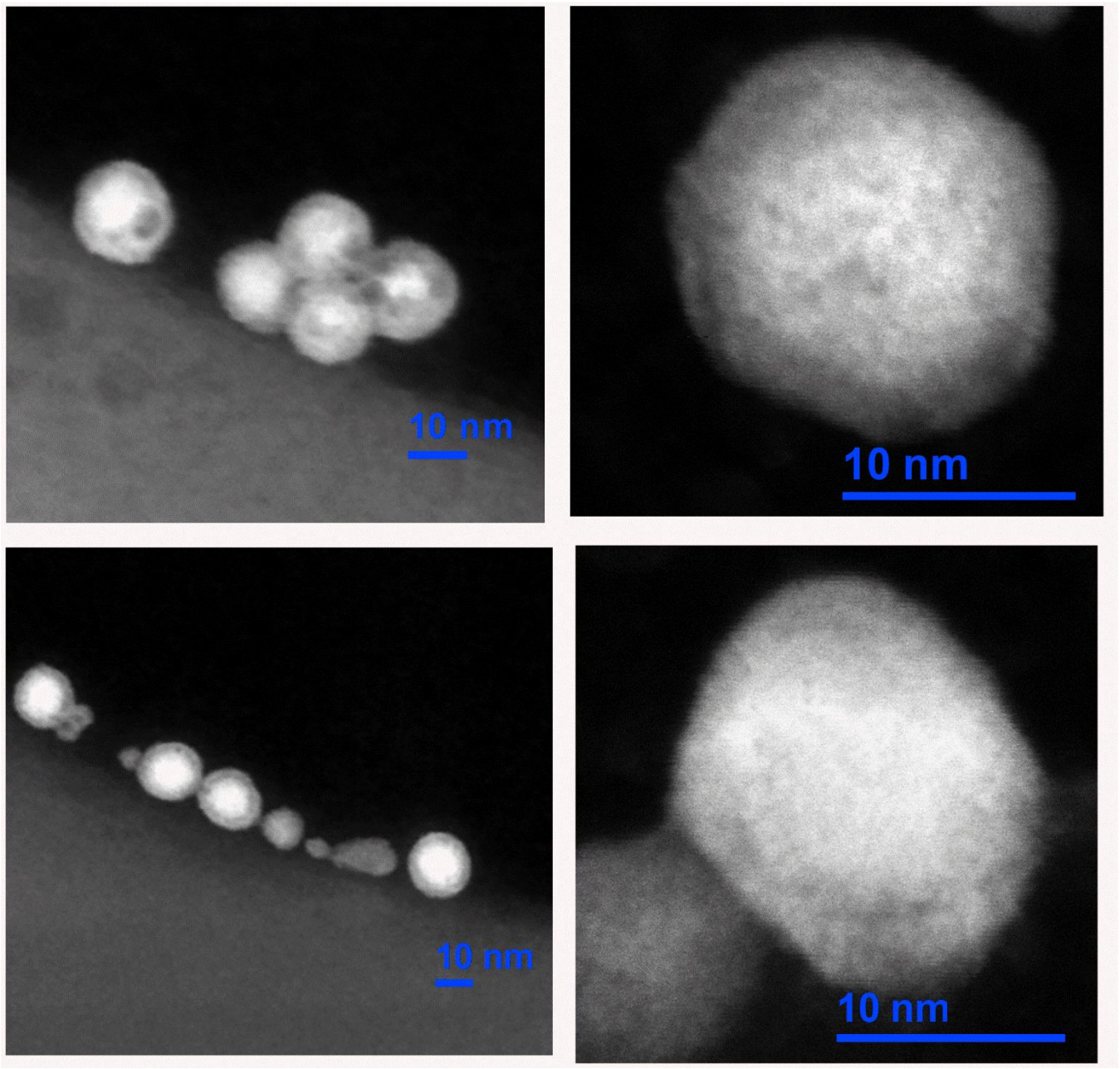

Figure S4. High Angle Annular Dark Field-STEM (HAADF-STEM) images of the α-$NaY_{0.85}Dy_{0.15}F_4$@ α-$NaYF_4$@β-$NaGd_{0.80}Er_{0.02}Yb_{0.18}F_4$ @β-$NaGd_{0.75}Nd_{0.25}F_4$ core@*multi*-shell nanoparticles

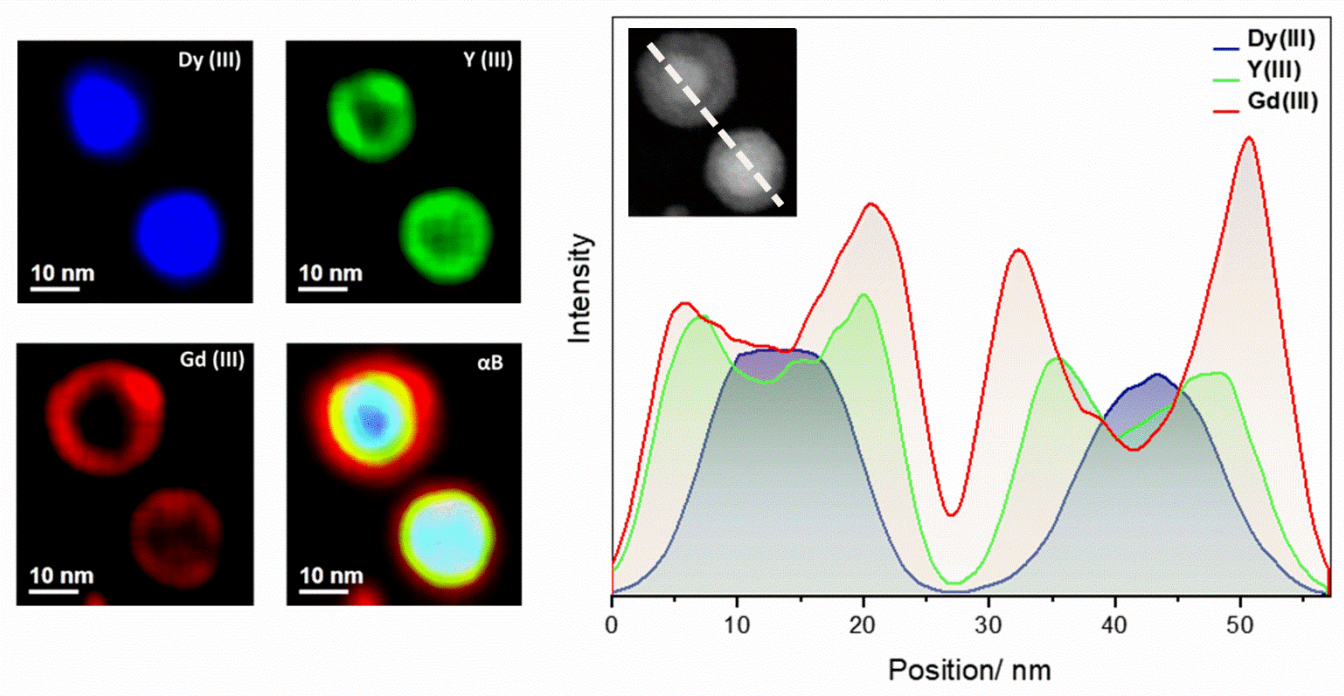

Figure S5. (A) EDS elemental mapping of the α-$NaY_{0.85}Dy_{0.15}F_4$@$NaYF_4$@β-$NaGd_{0.80}Er_{0.02}Yb_{0.18}F_4$ @$NaGd_{0.75}Nd_{0.25}F_4$ core@multi-shell nanoparticles and (B) Distribution profile of Dy^{III} (blue), Y^{III} (green) and Gd^{III} (red) ions along the α-$NaY_{0.85}Dy_{0.15}F_4$@ α-$NaYF_4$@β-$NaGd_{0.80}Er_{0.02}Yb_{0.18}F_4$ @β-$NaGd_{0.75}Nd_{0.25}F_4$ core@multi-shell nanoparticles.

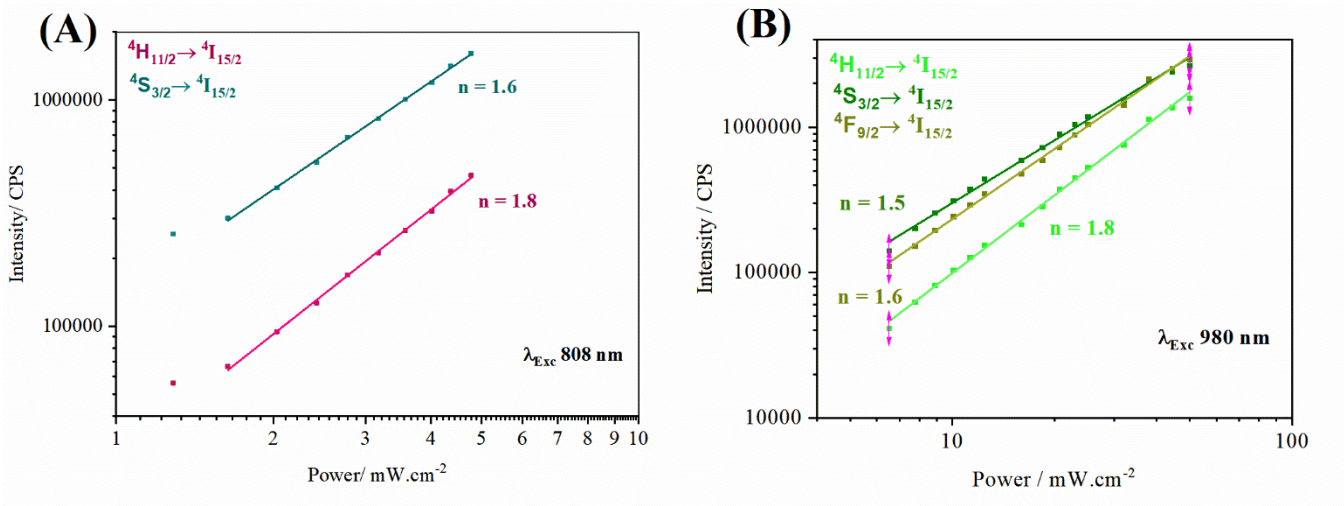

Figure S6. Emission intensities versus excitation power of Er^{III} ion ($^4H_{15/2}\rightarrow {}^4I_{15/2}$, $^4S_{3/2}\rightarrow {}^4I_{15/2}$ and $^4F_{9/2}\rightarrow {}^4I_{15/2}$,) (A) excitation at 808 nm, (B) excitation at 980 nm of the α-$NaY_{0.85}Dy_{0.15}F_4$@ α-$NaYF_4$@β-$NaGd_{0.80}Er_{0.02}Yb_{0.18}F_4$ @β-$NaGd_{0.75}Nd_{0.25}F_4$ core@multi-shell nanoparticles.

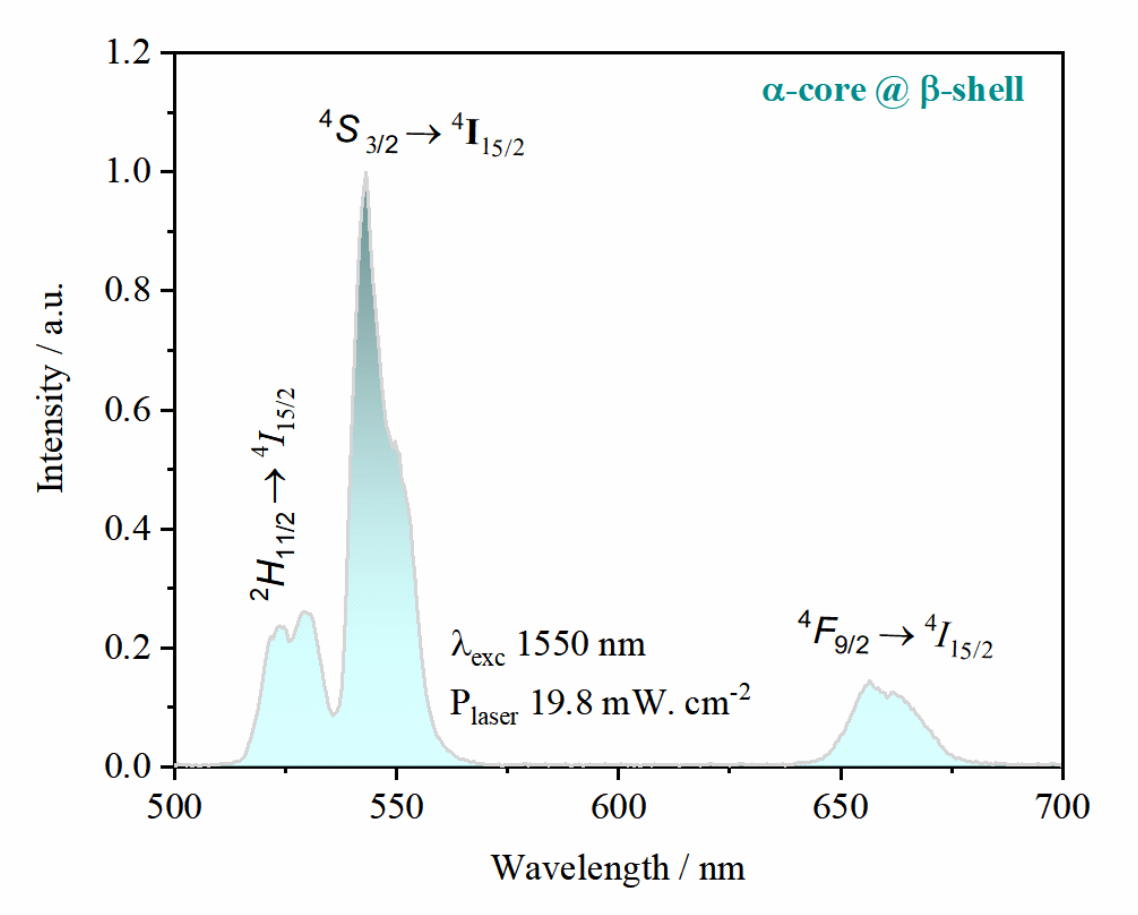

Figure S7. Upconversion luminescence spectra of α-$NaY_{0.85}Dy_{0.15}F_4$@α-$NaYF_4$@β-$NaGd_{0.80}Er_{0.02}Yb_{0.18}F_4$@β-$NaGd_{0.75}Nd_{0.25}F_4$ nanoparticles under laser excitation at 1550 nm (19.8 mW.cm^{-2}).

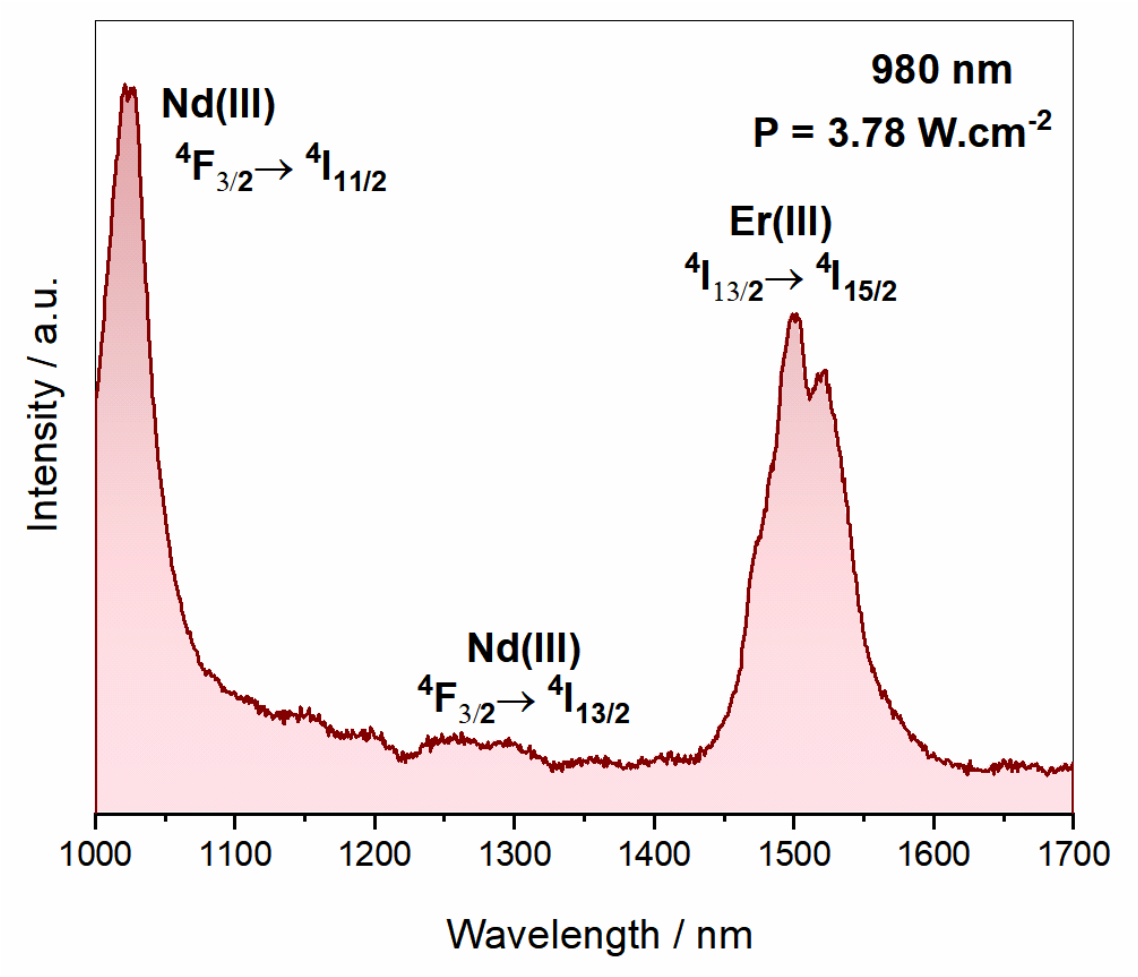

Figure S8. Downshifting luminescence spectra of the α-$NaY_{0.85}Dy_{0.15}F_4$@α-$NaYF_4$@β-$NaGd_{0.80}Er_{0.02}Yb_{0.18}F_4$@β-$NaGd_{0.75}Nd_{0.25}F_4$ nanoparticles under laser excitation at 980 nm (3.78 $mW.cm^{-2}$).

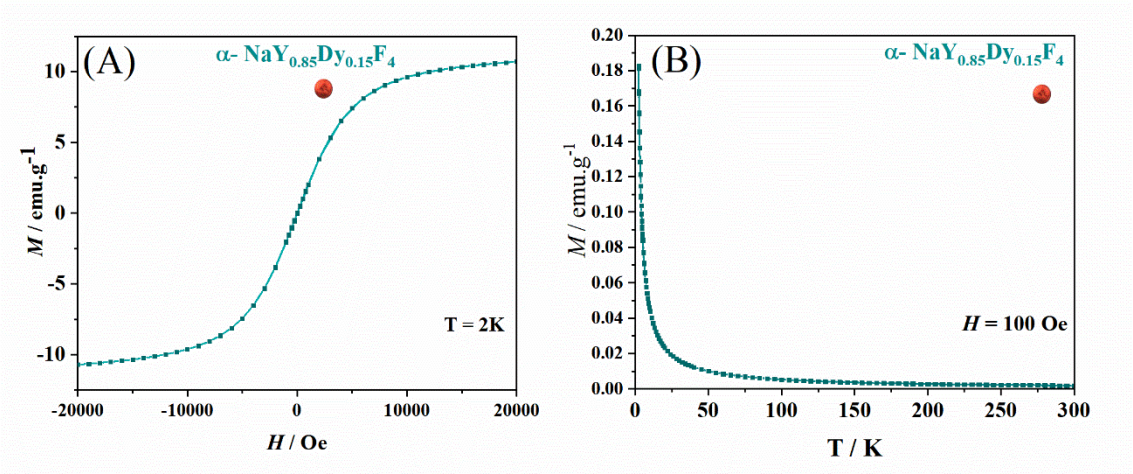

Figure S9. (A) Hysteresis experiments performed at 2 K and (B) Zero-field cool/field cool (ZFC/FC) experiment performed from 2 to 300 K using an applied field of 100 Oe of the α-$NaY_{0.85}Dy_{0.15}F_4$ core nanoparticles.